Nano Energy 132 (2024) 110377

Contents lists available at ScienceDirect

Nano Energy

journal homepage: www.elsevier.com/locate/nanoen

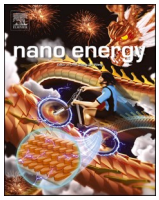

Self-powered intelligent badminton racket for machine learning-enhanced real-time training monitoring

Junlin Yuan [a,b,1], Jiangtao Xue [b,e,1], Minghao Liu [b,f], Li Wu [b,d], Jian Cheng [b,d], Xuecheng Qu [b,g], Dengjie Yu [b,h], Engui Wang [b], Zhenmin Fan [i], Zhuo Liu [b,c,*], Zhou Li [a,b,d,**], Yuxiang Wu [a,b,**]

[a] Institute of Intelligent Sport and Proactive Health, Department of Health and Physical Education, Jianghan University, Wuhan 430056, China
[b] Beijing Institute of Nanoenergy and Nanosystems, Chinese Academy of Sciences, Beijing 101400, China
[c] Key Laboratory of Biomechanics and Mechanobiology of Ministry of Education, Advanced Innovation Center for Biomedical Engineering, School of Engineering Medicine, Beihang University, Beijing 100191, China
[d] School of Nanoscience and Engineering, University of Chinese Academy of Sciences, Beijing 100049, China
[e] Institute of Engineering Medicine, School of Life Science Beijing Institute of Technology, Beijing 100081, China
[f] Department of Biomedical Engineering, The Chinese University of Hong Kong, 999077, Hong Kong SAR
[g] State Key Laboratory of Tribology in Advanced Equipment, Department of Mechanical Engineering, Tsinghua University, Beijing 100084, China
[h] Senior Department of Orthopedics, the Fourth Medical Center of PLA General Hospital, Beijing 100048, China
[i] School of Mechanical Engineering, Jiangsu University of Technology, Changzhou, Jiangsu, China

ARTICLE INFO

Keywords:
Intelligent sports
Self-powered
Intelligent badminton racket
Training monitoring
Machine learning

ABSTRACT

Intelligent sensing technology exerts a crucial role in badminton training: by capturing the behavior of athletes, the technology can effectively promote the enhancement of motor skills and performance. However, sports sensors that are multifunctional, real-time, and convenient remain an ongoing challenge. This study designs a self-powered intelligent badminton racket (SIBR) with machine learning-based triboelectric/piezoelectric effects. The silver paste coating method is employed for constructing customized electrodes, thereby forming triboelectric sensing array on the badminton strings, which enables hitting position monitoring. Meanwhile, flexible piezoelectric films with a specific shape are embedded in the hand glue; thus, the grip posture is identified. These sensing arrays can directly convert mechanical signals into electrical signals for achieving zero power consumption. In addition, the study integrates a wireless module for signal acquisition and transmission at the bottom of the racket handle, which ensures real-time sensor monitoring based on normal usage. The collected multi-channel data obtained from the SIBR is utilized for machine learning, achieving an accuracy of hitting position that can reach 95.0 %. SIBR provides a powerful reference for badminton training and unfolds a new path and direction for badminton sports monitoring.

1. Introduction

In recent years, sports sensing technology has developed rapidly. The demand for scientific and precise sports is gradually increasing, which also promotes the continuous updating and development of intelligent sports equipment. Intelligent sports technology effectively promotes scientific exercise: monitoring and analyzing sports data, users can more optimally understand their physical condition and exercise effects[1–4]. Badminton is a sport with many technical changes. Numerous factors determine the outcome of a match, among which technology is crucial and exerts a leading role. The correct hitting position is crucial for mastering badminton-related technical movements in practice[5]. An athlete's grip posture and strength, body posture, and swing speed may impact the hitting shuttlecock's position and strength. Different

* Corresponding author at: Key Laboratory of Biomechanics and Mechanobiology of Ministry of Education, Advanced Innovation Center for Biomedical Engineering, School of Engineering Medicine, Beihang University, Beijing 100191, China.
** Corresponding authors at: Institute of Intelligent Sport and Proactive Health, Department of Health and Physical Education, Jianghan University, Wuhan 430056, China.
E-mail addresses: liuzhuo@buaa.edu.cn (Z. Liu), zli@binn.cas.cn (Z. Li), yxwu@jhun.edu.cn (Y. Wu).
[1] These authors contributed equally to this work.

https://doi.org/10.1016/j.nanoen.2024.110377
Received 29 August 2024; Received in revised form 5 October 2024; Accepted 15 October 2024
Available online 22 October 2024

positions have different force transfer effects, and the optimal position maximizes energy transfer, leading to the most powerful hits. Meanwhile, the grip posture and grip strength directly affect the hitting position and strength, thereby affecting the quality of technical movements [6]. Therefore, continuously hitting the shuttlecock in the best position is a skill that should be practiced. Identifying the area with the highest power transmission efficiency and correcting the grip are key factors for improving badminton skills.

Virtual Reality (VR) imaging technology enables accurate monitoring of the hitting position[7]. However, because VR imaging technology has drawbacks such as high costs, complex processes, and demanding field requirements, it is difficult to implement in daily training. In recent years, research on badminton-applied sensors, which entails identifying and monitoring the swing trajectory, swing speed, hitting movements, and exercise load during the movement process, has gradually increased. Motion data was collected by attaching accelerometers and gyroscopes to the bottom of the badminton racket handle, and technical movements were identified through model processing[8]. Moreover, a body sensing network system was constructed by four wireless inertial sensor nodes, which were placed on the left arm, right arm, waist, and right ankle to explore the recognition of different hitting movements performed by badminton players[9]. Although this type of sensor describes the research direction for badminton motion sensing, its monitoring indicators are limited, and most of them should be worn on different parts of the body, which is quite inconvenient. Therefore, in the field of badminton motion sensing, the development of such equipment should still prioritize intelligence, miniaturization, and convenience.

Traditional sensors require energy storage devices (batteries) for power supply. The utilization of batteries exhibits drawbacks such as limited life, high replacement costs, and environmental pollution. Moreover, because the large volume of some intelligent sports devices and sensors is mainly due to the presence of batteries, the entire system is inconvenient and difficult to integrate. Therefore, developing a self-powered sensing system that is easy to integrate with sports equipment is particularly crucial for the development of intelligent sports. In 2012, Zhong Lin Wang's team developed a triboelectric nanogenerator [10]. Its basic principle is based on the coupling effect of contact electrification and electrostatic induction[11]. In addition, Zhong Lin Wang's team, who also invented the piezoelectric nanogenerator, proposed the original concept and basic theory of piezoelectric electronics, and formed corresponding research fields[12]. The device operates as a self-powered sensor for sports sensing by converting mechanical signals into electrical signals. This sensor, which based on the triboelectric effect and piezoelectric effect, provides a feasible solution to the energy supply problem[13–15]. Nanogenerator self-powering technology exhibits immense potential in fields pertaining to objects such as smart wearable devices, and health monitoring equipment[1,16–18]. The technology is low cost, exhibits a flexible size, is portable, includes diverse materials, and is widely applied[19,20]. These types of sports facilities and wearable devices are widely utilized in sports such as running, table tennis, skiing, golf, boxing, rope skipping, and swimming [21–23].

This study reports intelligent badminton racket strings based on the triboelectric effect and a smart badminton racket handle based on the piezoelectric effect, and develops a self-powered intelligent badminton racket (SIBR) for machine learning-based training. The technique and method of constructing electrodes on badminton strings and installing (polyvinylidene difluoride) PVDF piezoelectric film sensors on the badminton racket handle make it possible to monitor the hitting position and grip posture in real- time without changing the structure and normal usage of the badminton racket itself. In addition, the technology can provide feedback on the hitting power and grip strength through electrical signals. Morever, the wireless module installed at the bottom of the badminton racket handle can transmit and process the collected 10-channel sensing signals. Subsequently, after undergoing machine learning, the data yields an accuracy rate of up to 95 % for determining the hitting area position on the badminton racket surface.Furthermore, integrating machine learning capabilities facilitates pattern recognition and refinement, and enhances accuracy in determining hitting area points on the racket face, thereby optimizing training effectiveness and performance assessment. By analyzing the collected electrical signal data and characteristics, individuals can obtain information such as the relative hitting force and grip force acting on the racket surface of the badminton racket. The monitoring of this series of sports indicators can enable the exerciser to clearly understand their training process and results, which provides a powerful reference for more rational and efficient badminton technology learning, training, and guidance. This work has unfolded a novel research direction for the intelligent sports self-powered sensing system in badminton and a novel vision and direction.

2. Results and discussion

2.1. Design and structure of SIBR

In badminton, the standard shuttlecock used in professional play is made of 16 overlapping feathers, typically from a goose or duck, embedded into a rounded cork base. The feathers are carefully selected and arranged to ensure consistent flight and aerodynamics. The cork base is usually covered with thin leather to enhance durability and provide a smooth surface for hitting. Fig. 1a depicts the material that was utilized to wrap the head of the shuttlecock polyurethane in a commonly utilized shuttlecock. The badminton string comprises an inner core and an outer wrapping layer. The most commonly utilized badminton string is YONEX's BG-65. The string's core material is multilayer resin, and the outer layer material is chemical synthetic resin braided fiber. A layer of metal conductive paint silver is platted on the strings. Due to the intersecting main strings and cross strings in the string net of a badminton racket, a metal single electrode with a sheet-like area can be formed. When the shuttlecock head comes into contact with the strings coated with conductive paint silver, the friction between the two materials generates an electrical signal based on the different frictional electrical sequences[24–26]. This electrical signal can be utilized to sense which area the shuttlecock is hitting and to identify the hitting point. The piezoelectric unit of the badminton racket handle utilizes a PVDF film, which exhibits a high piezoelectric coefficient, wide frequency response range, high stability, and favorable mechanical properties[27]. A Bluetooth electronic unit is installed at the bottom of the handle for signal acquisition and processing, and the unit subsequently transmits them to the computer display, which enables real-time display and feedback throughout the entire monitoring and training process. Fig. 1b depicts the process of processing, learning, identifying, and classifying electrical signals collected by SIBR. In preprocessing, the researchers extract some features from a raw signal each channel, including average, maximum and minimum, integration, standard deviation, entropy, and energy of signals. Using the extracting feature, researchers can encode signals and derive specific parameters that can be utilized to detect differences by model. The deep machine-learning process is detailed in the experimental section.

2.2. Fabrication and characterization of a triboelectric sensor array for badminton strings

In badminton, accurately hitting specific points (sweet spots, as shown in Fig. S1) on the racket surface can enhance the shuttlecock's accuracy. Sweet spots are the central area of the badminton racket face, typically located near the intersection of the longitudinal and cross strings. Sweet spots generally cover approximately 25–35 % of the total racket face area, centered around the geometric midpoint. When players hit the shuttlecock in the sweet spot, they can control the shuttlecock's direction and spin with more ease, thereby reducing the likelihood of

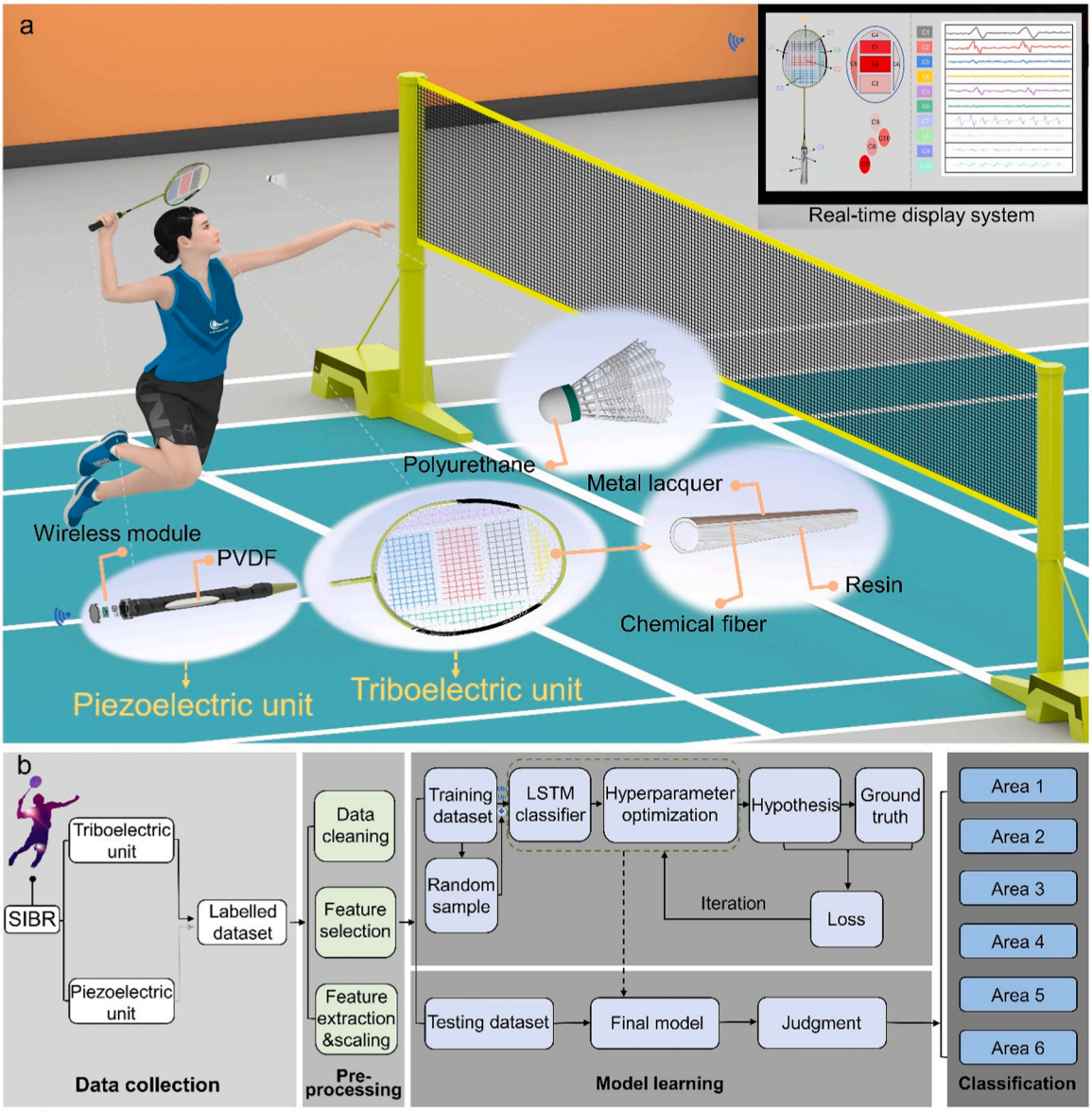

Fig. 1. Design and structure of a self-powered intelligent badminton racket (SIBR) for badminton training. (a) Schematic diagram of the SIBR and real-time display interface. (b) Machine learning workflow diagram.

mistakes. The accurate hitting point on the racket surface can enable players to more optimally comprehend the strength of the hit. By hitting the shuttlecock in the sweet spot, players can more accurately control the speed of the shuttlecock and avoid losing control (a phenomenon occasioned by excessive or insufficient force). Hitting the shuttlecock in the sweet spot enables the racket surface to fully harness its elasticity and provide greater rebound, thereby increasing the shuttlecock's speed and power[5,6]. This phenomenon is crucial for quick and powerful attacks during the playing process. Therefore, the racket surface is divided into six areas (Fig. 2a). Areas 1 and 2 almost cover the sweet area are situated approximately within the upper and lower parts of the sweet area respectively. The remaining areas 3, 4, 5, and 6 are non-sweet areas. Fig. 2b indicates that the original badminton string is insulated. Two identical mask plates are placed on the surface of the badminton racket. The mask plates are laser cut from the acrylic plate. Fix the mask plate symmetrically up and down, and spray the metal conductive silver paint. After spraying, remove the mask plate, and let it sit for 10 hours to air dry; thus, the badminton strings with metal electrodes are obtained. Observe a single badminton string before and after being coated with conductive paint under the scanning electron microscope. The internal structure of the badminton string and the difference in external morphology before and after coating with conductive paint can be clearly observed. Because the rigidity of the badminton string is weak, its cross-section is not a regular circle. Moreover, the imaging reveals that after spraying, the badminton string's surface is coated with a layer of metal conductive paint exhibiting a 14 μm thickness (Fig. 2c). Conductive silver particles are applied to the strings as conductive electrodes. To assess the impact of the 14 μm thin metal electrode layer on the elasticity of the badminton string, we measured the modulus of the string before and after electrode plating (Fig. S2). The results indicate that the modulus remained nearly unchanged, suggesting that the thin electrode layer does not significantly affect the string's elasticity or the quality of the shot. Fig. 2d indicates that when a shuttlecock comes into contact with strings coated with metal Ag electrodes, two different materials rub against each other, and the interaction between their atoms leads to the transfer of electrons. One of the materials loses electrons (carrying a positive charge), whereas the other material gains these electrons (carrying a negative charge). When charge separation

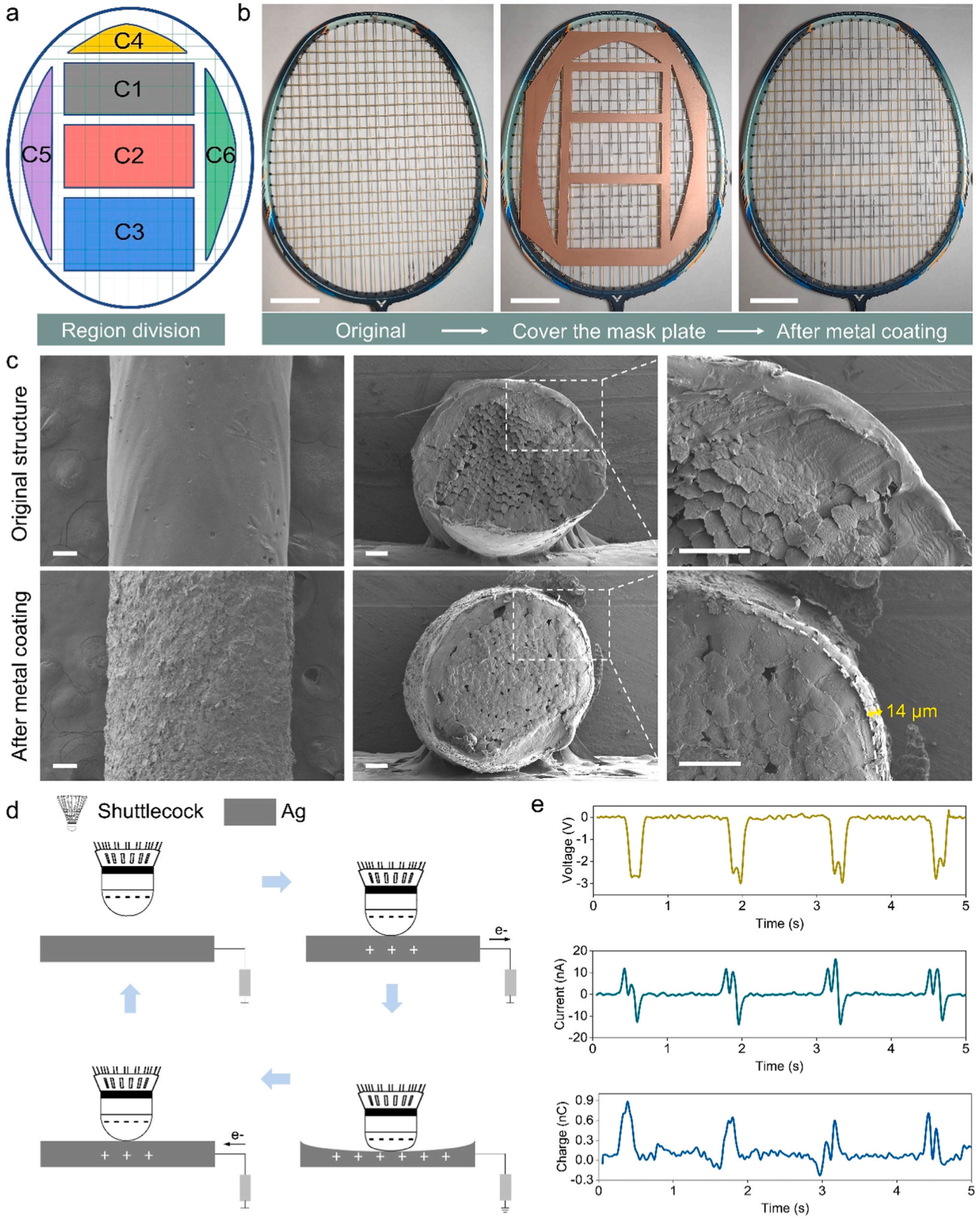

Fig. 2. Preparation process, principle and electrical output performance of badminton strings based on triboelectric effect. (a) Schematic diagram of the sensor-array division on the badminton racket's surface. (b) An illustration of badminton strings before and after spraying metal conductive paint (All scale bars in this figure represent 50 mm). (c) Badminton string surface and cross-section before and after spraying the metallic conductive paint imaged under a scanning electron microscope (All scale bars in this figure represent 200 μm). (d) Schematic diagram of the triboelectric effect principle. (e) The V_{OC}, I_{SC}, and Q_{SC} of a single-electrode triboelectric nanogenerator on badminton strings.

occurs in a material, it creates a voltage difference between the electrodes, thus forming an electric potential difference[28].

To characterize the electrical properties of this single-electrode TENG, the researchers tested its open circuit voltage (V_{OC}), short circuit current (I_{SC}), and transferred charge. Fix the shuttlecock on the linear motor, and place the racket surface vertically below the linear motor (Fig. 3a). A linear motor is utilized to hit the strings of a badminton racket at the same speed and displacement, thus simulating the electrical signal generated by the friction attributed to the shuttlecock hitting the strings at the same frequency and force. V_{OC} approximates 3 V, I_{SC} approximates 15 nA, and the transferred charge approximates 0.9 nC (Fig. 2e). The researchers utilized different lifting and lowering speeds of a linear motor to simulate the open circuit voltage of a shuttlecock hitting the strings at different frequencies (0.5–3 Hz). As the frequency increases, V_{OC} increases from 1 V to 5 V (Fig. S3a), which can be rationalized as follows: at lower frequencies (0.5–3 Hz), each contact and separation has sufficient time for thorough charge transfer, which is more conducive to effective charge transfer and accumulation. Therefore, the increase in voltage is more noticeable, resulting in an increase in voltage as the frequency increases[24,29]. To adjust the distance(0–21 mm), utilize different distances when the linear motor drops; the shuttlecock continues to fall after contact with the strings, thereby simulating the open circuit voltage of the shuttlecock hitting the strings at different strengths. As the falling distance

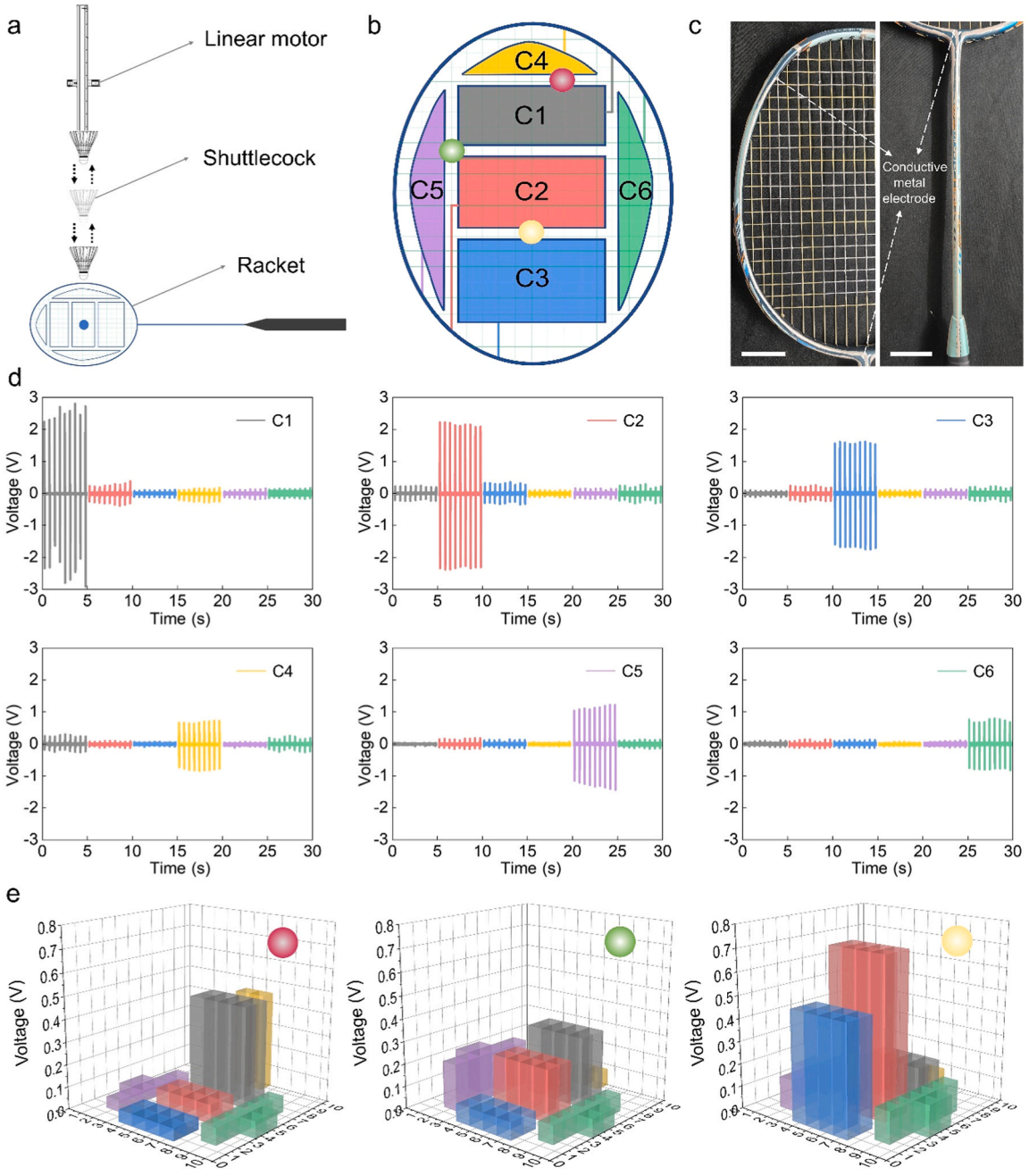

Fig. 3. Characterization of triboelectric signals from a multi-channel sensing array on a badminton racket surface. (a) Schematic diagram of a linear motor driving a shuttlecock to hit a badminton string. (b) Schematic diagram of the badminton string electrodes leading to the badminton racket frame and the shuttlecock hitting the edges of different areas simultaneously. (c) An illustration of the electrodes on the badminton string leading to the badminton racket frame and finally to the racket handle (All scale bars in this figure represent 40 mm). (d) Characterization of electrical signals using linear motors to hit the middle of a single area. **e** Characterization of electrical signals using linear motors to hit the edges of multiple areas.

continually increases, the open circuit voltage increases from 1 V to approximately 2 V (Fig. S3b), which can be explained as follows: the contact area increases when falling. The increase in the contact area between two different materials indicates that more atoms or molecules are involved in the charge separation process. As more material comes into contact, the opportunities for electron transfer and charge separation increase, thus leading to more positive and negative charges being separated during the friction process. These charges can accumulate between the electrodes, forming a higher charge density. Higher charge density leads to larger voltage differences. We utilized a linear motor to hit Area 2 on the badminton racket surface at a 1 Hz frequency for 10000 seconds, which is 10000 times. The V_{OC} stabilized at approximately 3.6 V and exhibited a satisfactory value (Fig. S4).

In addition, this study has converted the relationship between the force on the badminton string and the open circuit voltage. Commercially available resistive sensors were connected to an electrostatic voltmeter; thus, a constant voltage source was established. With respect to positioning the sensors beneath the shuttlecock line to ensure alignment with contact points, shuttlecocks were vertically secured on a Mark-10 digital force gauge, with adjustments made to align the head precisely with the sensors. Forces of varying magnitudes were applied using the Mark-10 force gauge, with corresponding currents recorded by the voltmeter. Using curve fitting, the researchers determined the relationship between force and resistance (Fig. S5a). Subsequently, they connected the resistive sensors to the voltmeter and fixed the shuttlecock on the vertical axis of a linear motor. By recording currents induced by forces under different motor parameters, the researchers could calculate resistance values. Utilizing established force-resistance relationships, they precisely calculated forces applied by the linear motor under various settings. Subsequently, the researchers conducted striking experiments on the racket using identical linear motor parameters and recorded voltage signals with an oscilloscope. This step enabled them to establish a relationship between applied force and resultant voltage (Fig. S5b).

To realize that there are no wires on the badminton strings and to avoid affecting the normal usage of the badminton racket during competition or training, a method of guiding the wire was designed. There is a 8–10 mm gap between two adjacent areas, and the strings in this gap are not plated with metallic conductive paint. Therefore, the researchers painted metal conductive paint silver along a string in the gap, and after painting, the string was not connected to any area between the two adjacent areas. Finally, the conductive metal paint leads along a badminton string to the edge of the badminton racket frame (Fig. 3b), which can be rationalized as follows: the surface of the normal badminton racket frame and racket stick is insulating and non-conductive. Therefore, the conductive paint is led to the edge of the badminton racket frame and continues down along the badminton racket frame and stick shaft. Six long strips of conductive paint leading from six different areas act as wires. Finally, it is led to the top of the badminton racket handle, and the six long strips of conductive paint do not cross each other (Fig. 3c).

Based on the fixed frequency and displacement of the linear motor hitting the badminton string, the study collected and characterized the multi-channel signals when hitting six different areas (Fig. 3d). Under the same experimental conditions, hitting different areas exhibits apparent signal characteristics. Furthermore, when it hits the middle area, the open circuit voltage is relatively large, especially in areas 1 and 2. This observation may be explained as follows: these two areas are the sweet spots on the badminton racket surface. Because the badminton string in the sweet zone exhibits the greatest elasticity, the vibration that occurs when hitting the badminton string is greater, and the contact may be more complete; thus, the triboelectric effect is greater, and the open circuit voltage is higher. The study also conducted tests by hitting multiple areas simultaneously (the edges of multiple areas) and characterized the data (Fig. 3e). The three hitting positions correspond to the positions illustrated in Fig. 3b. It can be observed from the data plot that the open circuit voltage is significantly smaller when hitting the edges of multiple areas. However, there are also apparent signal characteristics, and the location of the hit can be determined based on the electrical signal characteristics. Therefore, whether the shuttlecock hits a certain area or multiple areas, the sensing array can determine and identify the hitting location based on the electrical signal characteristics.

2.3. Fabrication and characterization of a piezoelectric sensor array on the handle of badminton racket

Based on the piezoelectric nanogenerator principle, the researchers built a four-channel piezoelectric sensing array on the racket handle, using commercially available silver-coated PVDF piezoelectric films. The piezoelectric effect of PVDF is based on changes in its crystal structure. PVDF has different crystal phases, among which the β phase (the most common piezoelectric phase) exhibits higher piezoelectric properties. In PVDF, the orientation of the molecular chains is modified, leading to positive polarization (the molecular chains face the same direction) and negative polarization (the molecular chains face the opposite direction). This polarization phenomenon is occasioned by the uneven distribution of fluorine atoms (F) and hydrogen atoms (H) in the PVDF molecules, leading to the formation of a dipole moment[30]. When external pressure is applied, the PVDF-based molecular chains become displaced, leading to positive and negative polarization phenomena. As pressure is applied, the PVDF film deforms, which induces a scenario in which the charge distribution between the silver change (Fig. 4a). This change in charge distribution is the piezoelectric effect (the PVDF film generates charges when it is acted upon by external forces), thereby achieving the piezoelectric effect. For the PVDF piezoelectric film sensor in this study, the generated output voltage gradually increased from 1.12 V to 3.89 V when the applied pressure ranged from 2 to 90 N (2.83–127.39 kPa) (Fig. S6). The force-voltage relationship exhibited a clear linear trend. We performed a linear fit on the data, and the slope of the fitted line was taken as the sensor's sensitivity, which is 0.0229 V/kPa. This sensitivity is comparable to that of previously reported related PVDF piezoelectric sensors[31,32]. And because PVDF is very flexible, it fits perfectly between the handle of a badminton racket and the grip that wraps the handle. Therefore, the application of PVDF piezoelectric film sensors will not affect the badminton sport itself, and has good sensitivity. In addition, the response time of the PVDF piezoelectric sensor was measured using voltage waveform data, resulting in a response time of 0.04861 seconds (Fig. S7). The study utilized a linear motor to simulate the open circuit voltage of the piezoelectric sensor when pressing the racket handle at different frequencies (0.5–2 Hz). As frequency increases, V_{OC} increases from 1.8 V to 3 V (Fig. S8a), which is related to the matching of molecule/crystal vibrational frequencies. The piezoelectric effect is occasioned by vibrations of the molecular or lattice structure within the material. The piezoelectric effect is maximized when the externally applied frequency matches the natural frequency of the material's internal molecular or lattice vibrations. Therefore, as the frequency increases, it is easier for the external vibration to match the vibration frequency of the molecules or lattice inside the material, which induces a stronger piezoelectric effect[33]. In addition, high-frequency vibration can induce a scenario where the strain rate inside the material increases. Increasing the strain rate induces greater polarization charge distribution inhomogeneity, ultimately leading to a greater open circuit voltage. The piezoelectric effect is most significant when the external vibration is in phase with the vibration of the molecules or lattice inside the material. High-frequency vibrations are usually more likely to be in phase with the vibrations inside the material in this case, the piezoelectric effect is enhanced, and the open circuit voltage becomes larger[34]. Utilize different distances when the linear motor descends; to adjust the distance (0–10 mm), the motor continues to descend after contacting the piezoelectric sensor, thereby simulating the open circuit voltage under different gripping strengths. As the descent distance increases, the open circuit voltage increases from nearly 0 to

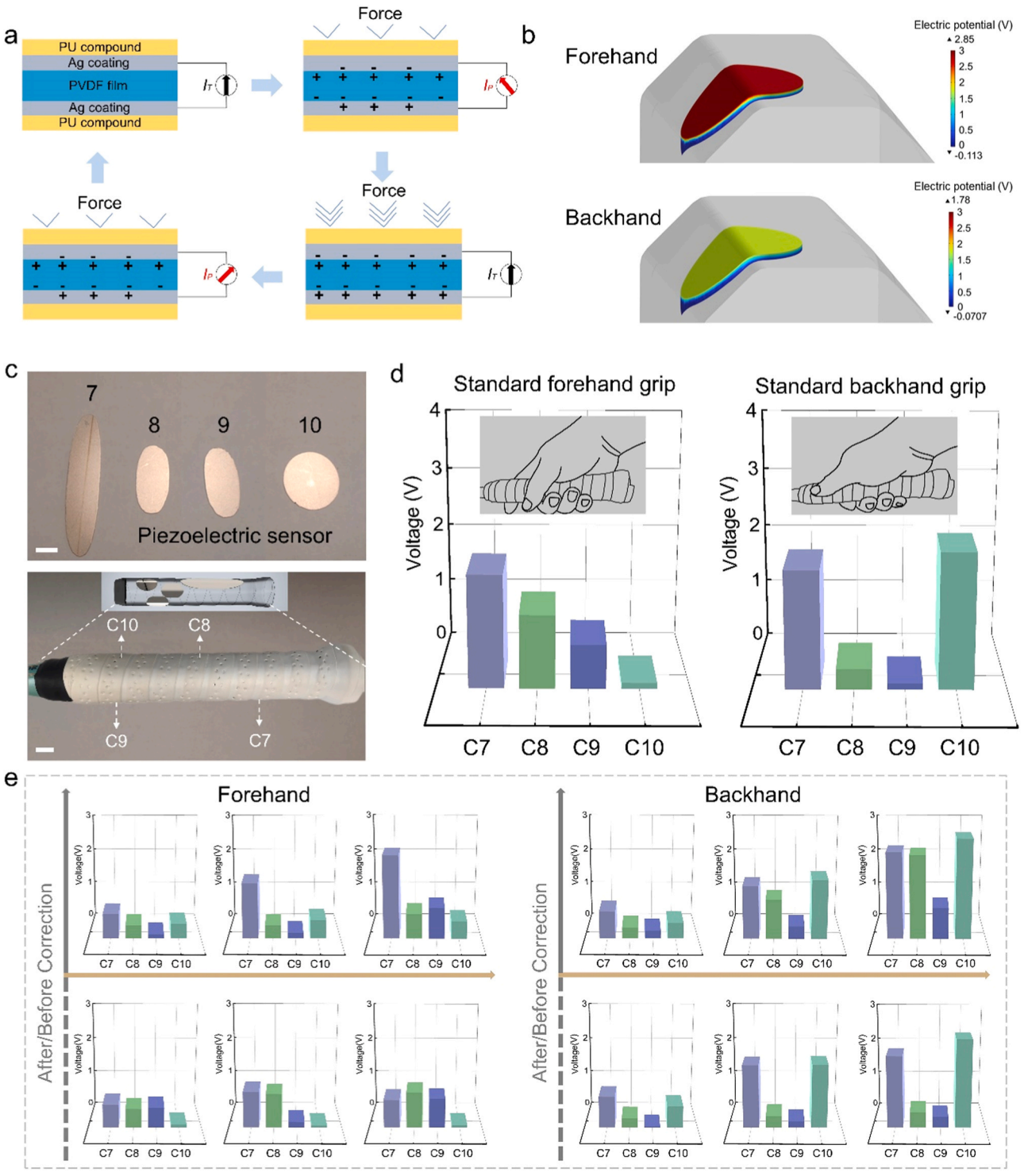

Fig. 4. Mechanism of piezoelectricity sensing and sensor performance characterization. (a) Schematic diagram of the piezoelectric-effect principle. (b) Simulation diagram that depicts the forehand grip's and backhand grip's stress. (c) The shape, size, and position of the PVDF piezoelectric thin film, and the actual and schematic diagram of the badminton racket handle wrapped in grip tape (All scale bars in this figure represent 10 mm). (d) Electrical signal characteristics of the standard forehand grip and backhand grip in badminton. (e) The electrical signal characteristics of a badminton amateur (without receiving badminton education or training) before and after correcting the forehand and backhand grip.

approximately 3 V (Fig. S8b), which can be explained as follows: as the pressure increases, the piezoelectric material's degree of molecular or lattice displacement also increases, thus inducing an increase in polarization. In piezoelectric materials, the more polarized the molecules, the greater the potential difference produced, thereby leading to an increase in the open circuit voltage[35]. In addition, the increase in pressure leads to a scenario in which the charge density inside the material increases. As a material's charge density increases, the current generated also increases, thus enhancing the piezoelectric effect[36]. The electrical potential distribution on the badminton racket handle was simulated using COMSOL Multiphysics (Fig. 4b). The finite element model was created based on the geometry of the racket handle and the piezoelectric

sensor, with appropriate material properties assigned. Boundary conditions were applied to simulate typical grip forces during play. The simulation focused on the electric potential generated by the sensor under these conditions, illustrating its ability to effectively monitor grip pressure and performance.

According to the position of the fingers pressed when holding the racket forehand and backhand in badminton, as well as the shape and size of the badminton racket handle, the study designed four piezoelectric sensors: one 60×15 mm ellipse, two 30×15 mm ovals, and one 25×25 circle (Fig. 4c). This design just fits the difference in fingers and positions when holding the badminton racket forehand and backhand. Specifically, it is three fingers or four fingers, thumb, index finger, and thumb. These four piezoelectric sensors are fixed at four positions on the badminton racket handle. The position of the piezoelectric sensor is

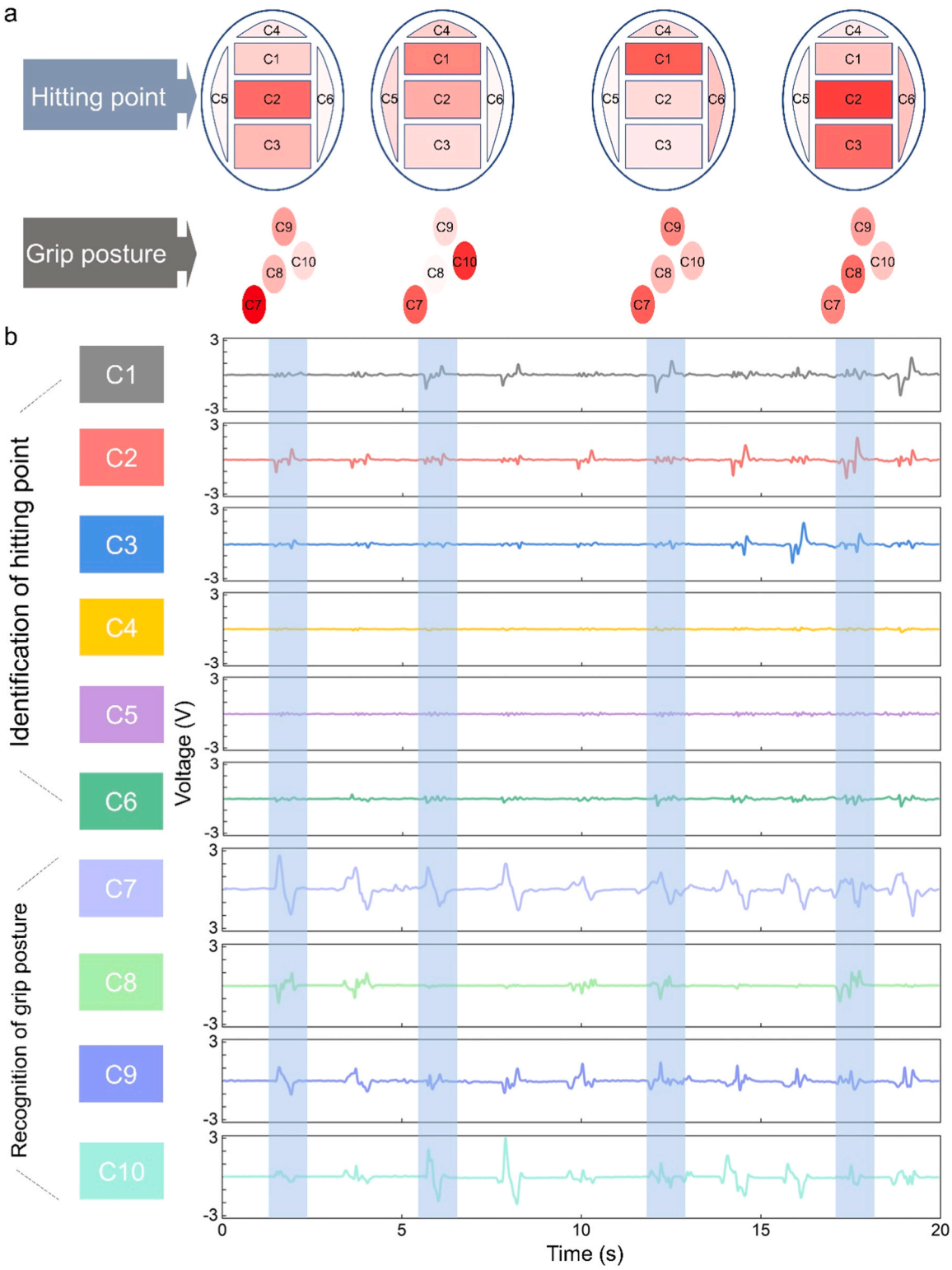

Fig. 5. Ten-channel sensing system for monitoring badminton training process. (a) The display results of identifying the hitting position and grip posture based on the analysis of ten-channel wired test signals. (b) Characterization of tests on a ten-channel wired system for monitoring badminton training processes.

stabilized under the badminton hand glue and does not affect normal usage. According to the position of the piezoelectric sensor designed herein, when the athlete utilizes a standard badminton forehand grip, three fingers are pressed on sensor 7, the thumb is pressed on sensor 8, and the index finger is pressed on sensor 9. Thus, the three channels 7, 8, and 9 will have exhibit significant piezoelectric signals. When the athlete uses utilizes a standard badminton backhand grip, four fingers press on sensor 7 and the thumb presses on sensor 10. Thus, the two channels, namely 7 and 10, exhibit significant piezoelectric signals (Fig. 4d). After testing by 10 volunteers (all beginners or enthusiasts of badminton who have never experienced systematic learning) under the guidance of badminton majors from the Institute of Physical Education, it was proved that this sensing array exhibits satisfactory universal applicability. Using the racket handle's piezoelectric sensor array, the forehand and backhand grips of badminton beginners or enthusiasts can be corrected based on signal characteristics. Fig. 4e depicts the test results of a badminton beginner before and after guidance and correction. In addition, the force exertion methods and habits of different

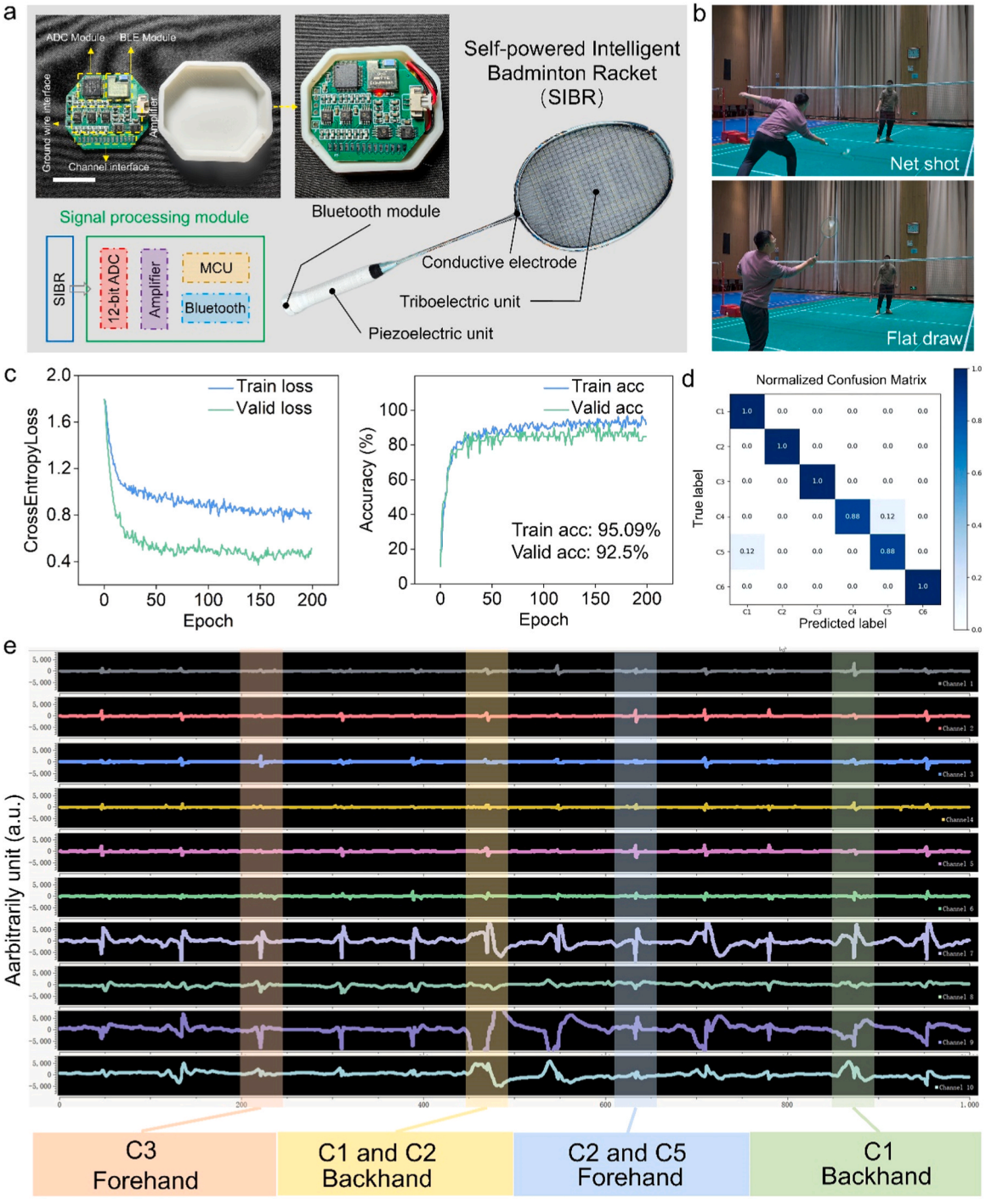

Fig. 6. Badminton training monitoring function assessment system based on SIBR. (a) Schematic diagram of the badminton training monitoring system and physical picture of the signal processing module (The scale bar in this figure represents 15 mm). (b) Optical photos of training monitoring using SIBR at a badminton court. (c) The classification results using LSTM. (d) Confusion matrix for predicting batting position through the machine learning model. (e) SIBR's computer interface display during application.

individuals can also be monitored and judged based on the size of the open circuit voltage; different channels of piezoelectric sensors correspond to different fingers holding the racket. Therefore, the racket handle sensor array can not only monitor and identify the grip posture through the signal characteristics of different channels, but also monitor and identify force- exerting habits based on the same channel's signal size. This kind of monitoring data can provide robust support for badminton players' grip posture and power-generating habits. We utilized a linear motor to simulate pressing a piezoelectric sensor 10000 times at a frequency of 1 Hz. V_{OC} is stable at approximately 1.9 V and exhibits satisfactory stability (Fig. S9).

2.4. System testing and applications

For sensing systems utilized in badminton training, it is of immense significance to stabilize the hitting position and grip posture during badminton practice. The accuracy of the hitting position directly affects the quality and direction of the hit. By monitoring the shot location, athletes can better adjust their body posture and movements to ensure that each shot is in the ideal position. The grip posture directly affects the shot's stability and accuracy. The correct grip posture can better exert force and enhance the control of the shuttlecock. Real-time monitoring provides athletes and coaches with the opportunity to improve technique and optimize training programs. By combining monitoring data with badminton sports learning models, personalized technical advice can be provided to athletes; thus, they can quickly enhance their skill levels. We utilized an oscilloscope to collect the ten-channel signals in a badminton match, which occurred on the badminton court. Data processing and result characterization are depicted in Fig. 5b. According to the signal strength of the six channels at the racket line, the hitting point can be distinguished and identified. According to the signal strength of the 4 channels at the handle, the grip posture can be distinguished and identified (Fig. 5a).

We developed a convenient badminton training monitoring system that does not affect the normal usage of badminton rackets or the normal movement of athletes. The system can monitor the hitting point and grip posture in real time and its composition block diagram, which includes four components:(PSTS, signal processing module, power management module, and desktop app), is illustrated in Fig. 6a. The specific system framework diagram is shown in Fig. S10. Moreover, the system's optical photo is depicted in Fig. 6a. The portable badminton training monitoring system can acquire real-time signals, which are subsequently processed and analyzed and finally displayed on a desktop application. The optical photo of the system when utilized in a badminton court is depicted in Fig. 6b. Different action techniques utilize different hitting points and grip postures. Using LSTM for classification, after 200 epochs, loss curve's convergence trend demonstrates that model is in a good fitting state, where accuracy attains more than 90 % (training set: 95.09 %, validation set: 92.5 %) as per Fig. 6c. Furthermore, the test set is also tested by a final model: its accuracy attains 95.0 %, and the corresponding confusion matrix is plotted in Fig. 6d. In addition, in actual combat, the SIBR application test was conducted on the badminton court, and its real-time display interface on the computer side is depicted in Fig. 6e. Moreover, after machine learning, SIBR can accurately feedback hitting information; the researchers selected 4 points and highlighted them to illustrate the SIBR recognition results after machine learning. The collected data corresponding to the display interface in Fig. 6e are characterized and depicted in Fig. S11. Additionally, the study conducted wireless system tests with six channels on the racket surface, four channels on the racket handle, and ten channels on the racket surface and handle. The corresponding demonstration videos can be identified in Video. S1, S2, and S3.

Supplementary material related to this article can be found online at doi:10.1016/j.nanoen.2024.110377.

3. Conclusions

In summary, this study demonstrates a self-powered intelligent badminton racket for machine learning-enhanced real-time training monitoring based on triboelectric and piezoelectric effects. As a self-powered sensor, the six-channel triboelectric sensing array can identify and monitor the hitting position through the contact between the strings and the shuttlecock at the surface of the badminton racket. Meanwhile, through the pressing patterns of different fingers on the handle, the four-channel piezoelectric sensor array can determine and identify the grip posture. The designed sensing system exhibits strong self-powering characteristics and does not require batteries. In addition, the researchers have built a wire-free sensing system for the entire badminton racket and integrated a wireless module for signal acquisition and transmission at the bottom of the racket handle. The utilization of the entire system ensures that it does not affect the process of badminton play. The collected SIBR-obtained multi-channel data is utilized for machine learning with a hitting- position accuracy of up to 95.0 %. SIBR has excellent energy collection and motion monitoring capabilities, which offer a powerful reference for badminton training and unfold novel paths and directions for badminton motion monitoring.

4. Experimental section

4.1. Fabrication of a badminton string sensing array

First, the prepared mask plates (made by laser cutting an acrylic plate) were placed on the racket surface of the badminton racket. The two mask plates were symmetrical installed up and down and fixed with tape. Subsequently, the conductive paint silver (Shenzhen Jingzhe Technology Co., Ltd.) was sprayed onto the badminton string in six areas that were not covered by the mask plates and was left to sit for ten hours; when the conductive paint dried, it firmly adhered to the badminton string, forming a stable six metal electrodes. Finally, the mask plates were removed, and a sensor array of six areas was formed on the badminton racket surface.

4.2. Fabrication of a sensing array at the handle of a badminton racket

First, the prepared PVDF piezoelectric film (Shenzhen Zhimk Technology Co., Ltd.) was cut into the shape illustrated in Fig. 4c by laser cutting. The piezoelectric sensor numbered 7 was 60×15 mm elliptical, the piezoelectric sensors numbered 8 and 9 were both 30×15 mm elliptical, and the piezoelectric sensor numbered 10 was 25×25 mm round. Subsequently, Kapton double-sided tape was utilized to attach the piezoelectric film to the handle of the badminton racket, and the positions of the four piezoelectric sensors were as depicted in the schematic diagram in Fig. 4c. Finally, a layer of grip tape was wrapped around the handle of the badminton racket, as illustrated in Fig. 4c.

4.3. Characterization and measurement

The open-circuit voltage was measured by an oscilloscope (HDO6104, Teledyne LeCroy); the short-circuit current and short-circuit charge were measured using an electrometer (6517, Keithley) and recorded by the oscilloscope (HDO6104, Teledyne LeCroy). A linear motor (E1100, Limo) was utilized to apply a periodic stable force on the FTTS for periodic testing such as electrical output performance characterization and fatigue test. A Scanning Electron Microscope (Nova NanoSEM 450) was utilized to observe the cross-sectional microstructure of the badminton string after spraying conductive paint silver. All optical photos were taken by the SLR (A7M3, Sony).

4.4. Process of deep learning based on Pytorch (version 1.11)

(1) Collect samples and label them individually. (2) Split the whole dataset (300 samples) into a training set (220 samples), validation set (40 samples) and test set (40 samples) randomly. (3) Prepare the GPU (cuda version 11.3) for acceleration and some libraries, such as Pytorch, sklearning, scikitplot, and scipy. (4) All data should be preprocessed: perform downsampling to 500 points; calculate their features, standardize the feature scale by calling MinMaxScaler method, which is imported from sklearn libraries to avoid huge loss; and convert them to tensor, and get prepared to training. (5) Encode label into one-hot map. (6) Define some important variables for training, including number of epochs = 200, learning rate = 0.0005, number of features = 7, hidden size = 64 (number of features in the hidden state), num layers = 2 (number of stacked LSTM layers), num classes = 6 (number of output classes), dropout = 0.2 to avoid overfitting, and GPU acceleration during Training loop; compute the cross loss between inputs and one-hoted label (CrossEntropyLoss), and improve the weights using an Adam optimizer step. (7) For better generalization abilities, Mix-Up methods are implemented, and random noises are applied in training to mix up two inputs and two one-hoted labels, respectively. Mix-up is a data augmentation technique used in deep learning that enhances the training process by randomly mixing two samples and their corresponding labels during training. Specifically, it combines the input vectors and labels according to a specific ratio, as shown below:

$$\widetilde{x} = \lambda x_i + (1-\lambda)x_j$$

$$\widetilde{y} = \lambda y_i + (1-\lambda)y_j$$

(x_i, y_i) and (x_j, y_j) are two samples. x_i, x_j are raw input vectors. y_i, y_j are one-hot label encodings. λ is a value from the Beta distribution, usual in the range (0, 1). In a nutshell, Mix-up extends the training distribution by linear interpolations of features so that lead to linear interpolations of the associated targets, resulting in robustness enhancement and reducing overfitting of model.

Authors contribution

J. Y. and J. X. contributed equally to this work. Y. W., Z. Li and Z. Liu supervised the project and designed the experiment. J. Y. and J. X. carried out the experiment and wrote the paper. J. Y., J. X., M. L., L. W., J. C. and X. Q. performed experimental measurement and data analyses. J. Y., J. X., D. Y., and E. W. and Z. F. took and processed the experimental photograph and video. All authors reviewed and commented on the manuscript.

CRediT authorship contribution statement

Dengjie Yu: Methodology, Investigation. **Xuecheng Qu:** Methodology, Investigation. **Jian Cheng:** Methodology, Investigation, Data curation. **Li Wu:** Methodology, Investigation, Formal analysis. **Minghao Liu:** Methodology, Investigation. **Jiangtao Xue:** Writing – original draft, Methodology, Formal analysis. **Junlin Yuan:** Writing – original draft, Resources, Methodology, Investigation, Formal analysis, Data curation. **Zhuo Liu:** Writing – review & editing, Supervision, Project administration, Funding acquisition, Conceptualization. **Yuxiang Wu:** Writing – review & editing, Supervision, Project administration, Funding acquisition, Conceptualization. **Zhou Li:** Writing – review & editing, Supervision, Project administration, Funding acquisition, Conceptualization. **Zhenmin Fan:** Methodology, Investigation. **Engui Wang:** Methodology, Investigation.

Declaration of Competing Interest

The authors declare that they have no known competing financial interests or personal relationships that could have appeared to influence the work reported in this paper.

Acknowledgments

The authors thank the support of National Key R&D Program of China (2022YFE011170), Science Fund for Distinguished Young Scholars of Hubei Province (2023AFA109), National Natural Science Foundation of China (82071970, 82372141, T2125003), Beijing Natural Science Foundation (L212010), Scientific and Technological Innovation Project of China Academy of Chinese Medical Sciences (No. CI2023C020YL), and the Fundamental Research Funds for the General Universities.

Appendix A. Supporting information

Supplementary data associated with this article can be found in the online version at doi:10.1016/j.nanoen.2024.110377.

Data Availability

Data will be made available on request.

References

[1] J. Luo, W. Gao, Z.L. Wang, The triboelectric nanogenerator as an innovative technology toward intelligent sports, Adv. Mater. 33 (2021) 2004178, https://doi.org/10.1002/adma.202004178.
[2] D. Yu, Z. Zheng, J. Liu, H. Xiao, G. Huangfu, Y. Guo, Superflexible and lead-free piezoelectric nanogenerator as a highly sensitive self-powered sensor for human motion monitoring, Nano-Micro Lett. 13 (2021) 117, https://doi.org/10.1007/s40820-021-00649-9.
[3] L. Zhao, X. Guo, Y. Pan, S. Jia, L. Liu, W.A. Daoud, P. Poechmueller, X. Yang, Triboelectric gait sensing analysis system for self-powered IoT-based human motion monitoring, InfoMat 6 (2024) e12520, https://doi.org/10.1002/inf2.12520.
[4] J. Xue, Y. Zou, Y. Deng, Z. Li, Bioinspired sensor system for health care and human-machine interaction, EcoMat 4 (2022) e12209, https://doi.org/10.1002/eom2.12209.
[5] T.-H. Liu, W.-H. Chen, Y. Shih, Y.-C. Lin, C. Yu, T.-Y. Shiang, Better position for the wearable sensor to monitor badminton sport training loads, Sports Biomechanics 1-13. https://doi.org/10.1080/14763141.2021.1875033.
[6] D.B. Waddell, B.A. Gowitzke, Gowitzke. Biomechanical principles applied to badminton power strokes, Engineering (2000). https://api.semanticscholar.org/CorpusID:107070024.
[7] X. Chu, X. Xie, S. Ye, H. Lu, H. Xiao, Z. Yuan, Z. Chen, H. Zhang, Y. Wu, TIVEE: visual exploration and explanation of badminton tactics in immersive visualizations, IEEE Trans. Vis. Comput. Graph. 28 (2022) 118–128, https://doi.org/10.1109/TVCG.2021.3114861.
[8] T. Steels, B. Van Herbruggen, J. Fontaine, T. De Pessemier, D. Plets, E. De Poorter, Badminton activity recognition using accelerometer data, Sensors 20 (2020) 4685, https://doi.org/10.3390/s20174685.
[9] Z. Wang, M. Guo, C. Zhao, Badminton stroke recognition based on body sensor networks, IEEE Trans. Hum. -Mach. Syst. 46 (2016) 769–775, https://doi.org/10.1109/THMS.2016.2571265.
[10] F.-R. Fan, Z.-Q. Tian, Z. Lin Wang, Flexible triboelectric generator, Nano Energy 1 (2012) 328–334, https://doi.org/10.1016/j.nanoen.2012.01.004.
[11] Z.L. Wang, J. Chen, L. Lin, Progress in triboelectric nanogenerators as a new energy technology and self-powered sensors, Energy Environ. Sci. 8 (2015) 2250–2282, https://doi.org/10.1039/C5EE01532D.
[12] Z.L. Wang, J. Song, Piezoelectric nanogenerators based on zinc oxide nanowire arrays, Science 312 (2006) 242–246, https://doi.org/10.1126/science.1124005.
[13] Y. Qin, X. Wang, Z.L. Wang, Microfibre–nanowire hybrid structure for energy scavenging, Nature 451 (2008) 809–813, https://doi.org/10.1038/nature06601.
[14] X. Wang, J. Song, J. Liu, Z.L. Wang, Direct-current nanogenerator driven by ultrasonic waves, Science 316 (2007) 102–105, https://doi.org/10.1126/science.1139366.
[15] Z.L. Wang, Nanopiezotronics, Adv. Mater. 19 (2007) 889–892, https://doi.org/10.1002/adma.200602918.
[16] X. Qu, J. Xue, Y. Liu, W. Rao, Z. Liu, Z. Li, Fingerprint-shaped triboelectric tactile sensor, Nano Energy 98 (2022) 107324, https://doi.org/10.1016/j.nanoen.2022.107324.
[17] H. Li, T. Chang, Y. Gai, K. Liang, Y. Jiao, D. Li, X. Jiang, Y. Wang, X. Huang, H. Wu, Y. Liu, J. Li, Y. Bai, K. Geng, N. Zhang, H. Meng, D. Huang, Z. Li, X. Yu, L. Chang, Human joint enabled flexible self-sustainable sweat sensors, Nano Energy 92 (2022) 106786, https://doi.org/10.1016/j.nanoen.2021.106786.
[18] R. Hinchet, H.-J. Yoon, H. Ryu, M.-K. Kim, E.-K. Choi, D.-S. Kim, S.-W. Kim, Transcutaneous ultrasound energy harvesting using capacitive triboelectric

technology, Science 365 (2019) 491–494, https://doi.org/10.1126/science.aan3997.
[19] W. Xu, H. Zheng, Y. Liu, X. Zhou, C. Zhang, Y. Song, X. Deng, M. Leung, Z. Yang, R. X. Xu, Z.L. Wang, X.C. Zeng, Z. Wang, A droplet-based electricity generator with high instantaneous power density, Nature 578 (2020) 392–396, https://doi.org/10.1038/s41586-020-1985-6.
[20] Y. Wu, Y. Li, Y. Zou, W. Rao, Y. Gai, J. Xue, L. Wu, X. Qu, Y. Liu, G. Xu, L. Xu, Z. Liu, Z. Li, A multi-mode triboelectric nanogenerator for energy harvesting and biomedical monitoring, Nano Energy 92 (2022) 106715, https://doi.org/10.1016/j.nanoen.2021.106715.
[21] J. Luo, Z. Wang, L. Xu, A.C. Wang, K. Han, T. Jiang, Q. Lai, Y. Bai, W. Tang, F. R. Fan, Z.L. Wang, Flexible and durable wood-based triboelectric nanogenerators for self-powered sensing in athletic big data analytics, Nat. Commun. 10 (2019) 5147, https://doi.org/10.1038/s41467-019-13166-6.
[22] K. Dong, J. Deng, W. Ding, A.C. Wang, P. Wang, C. Cheng, Y.-C. Wang, L. Jin, B. Gu, B. Sun, Z.L. Wang, Versatile core–sheath yarn for sustainable biomechanical energy harvesting and real-time human-interactive sensing, Adv. Energy Mater. 8 (2018) 1801114, https://doi.org/10.1002/aenm.201801114.
[23] Y. Zou, Y. Gai, P. Tan, D. Jiang, X. Qu, J. Xue, H. Ouyang, B. Shi, L. Li, D. Luo, Y. Deng, Z. Li, Z.L. Wang, Stretchable graded multichannel self-powered respiratory sensor inspired by shark gill, Fundam. Res. 2 (2022) 619–628, https://doi.org/10.1016/j.fmre.2022.01.003.
[24] T. Cheng, J. Shao, Z.L. Wang, Triboelectric nanogenerators, Nat. Rev. Methods Prim. 3 (2023) 39, https://doi.org/10.1038/s43586-023-00220-3.
[25] W.-G. Kim, D.-W. Kim, I.-W. Tcho, J.-K. Kim, M.-S. Kim, Y.-K. Choi, Triboelectric nanogenerator: structure, mechanism, and applications, ACS Nano 15 (2021) 258–287, https://doi.org/10.1021/acsnano.0c09803.
[26] Y. Yu, H. Li, D. Zhao, Q. Gao, X. Li, J. Wang, Z.L. Wang, T. Cheng, Material's selection rules for high performance triboelectric nanogenerators, Mater. Today 64 (2023) 61–71, https://doi.org/10.1016/j.mattod.2023.03.008.
[27] D. Hu, M. Yao, Y. Fan, C. Ma, M. Fan, M. Liu, Strategies to achieve high performance piezoelectric nanogenerators, Nano Energy 55 (2019) 288–304, https://doi.org/10.1016/j.nanoen.2018.10.053.
[28] Z. Zhang, Y. Bai, L. Xu, M. Zhao, M. Shi, Z.L. Wang, X. Lu, Triboelectric nanogenerators with simultaneous outputs in both single-electrode mode and freestanding-triboelectric-layer mode, Nano Energy 66 (2019) 104169, https://doi.org/10.1016/j.nanoen.2019.104169.
[29] Z.L. Wang, On Maxwell's displacement current for energy and sensors: the origin of nanogenerators, Mater. Today 20 (2017) 74–82, https://doi.org/10.1016/j.mattod.2016.12.001.
[30] A.J. Lovinger, Ferroelectric Polymers, Science 220 (1983) 1115–1121, https://doi.org/10.1126/science.220.4602.1115.
[31] J. Zhang, T. Yang, G. Tian, B. Lan, W. Deng, L. Tang, Y. Ao, Y. Sun, W. Zeng, X. Ren, Z. Li, L. Jin, W. Yang, Spatially confined MXene/PVDF nanofiber piezoelectric electronics, Adv. Fiber Mater. 6 (2024) 133–144, https://doi.org/10.1007/s42765-023-00337-w.
[32] W. Fan, R. Lei, H. Dou, Z. Wu, L. Lu, S. Wang, X. Liu, W. Chen, M. Rezakazemi, T. M. Aminabhavi, Y. Li, S. Ge, Sweat permeable and ultrahigh strength 3D PVDF piezoelectric nanoyarn fabric strain sensor, Nat. Commun. 15 (2024) 3509, https://doi.org/10.1038/s41467-024-47810-7.
[33] B. Mohammadi, A.A. Yousefi, S.M. Bellah, Effect of tensile strain rate and elongation on crystalline structure and piezoelectric properties of PVDF thin films, Polym. Test. 26 (2007) 42–50, https://doi.org/10.1016/j.polymertesting.2006.08.003.
[34] P. Sajkiewicz, A. Wasiak, Z. Gocłowski, Phase transitions during stretching of poly (vinylidene fluoride), Eur. Polym. J. 35 (1999) 423–429, https://doi.org/10.1016/S0014-3057(98)00136-0.
[35] A. Gaur, C. Kumar, S. Tiwari, P. Maiti, Efficient energy harvesting using processed poly(vinylidene fluoride) nanogenerator, ACS Appl. Energy Mater. 1 (2018) 3019–3024, https://doi.org/10.1021/acsaem.8b00483.
[36] R. Guo, H. Luo, X. Zhou, Z. Xiao, H. Xie, Y. Liu, K. Zhou, Z. Shen, L. Chen, D. Zhang, Ultrahigh energy density of poly(vinylidene fluoride) from synergistically improved dielectric constant and withstand voltage by tuning the crystallization behavior, J. Mater. Chem. A 9 (2021) 27660–27671, https://doi.org/10.1039/D1TA07680A.